Pergamon

PII: S0038–092X(01)00038–X

Solar Energy Vol. 69(Suppl.), Nos. 1–6, pp. 103–116, 2000

0038-092X/00/$ - see front matter

www.elsevier.com/locate/solener

OPTIMAL HEATING CONTROL IN A PASSIVE SOLAR COMMERCIAL BUILDING

MICHAËL KUMMERT, PHILIPPE ANDRɆ and JACQUES NICOLAS
Fondation Universitaire Luxembourgeoise, Avenue de Longwy, 185, B 6700 Arlon, Belgium

Received 20 June 2000; revised version accepted 16 February 2001

Communicated by VOLKER WITTWER

Abstract—A smart heating controller has a twofold objective: to save as much energy as possible while maintaining an acceptable comfort level in the building. Due to very large time constants in the building response, it has to anticipate internal and external disturbances. In the case of a passive solar commercial building, the need for anticipation is reinforced by important solar and internal gains. Indeed, large solar gains increase the energy savings potential but also the overheating risk. Optimal control theory presents an ideal formalism to solve this problem: its principle is to anticipate the building behaviour using a model and a forecasting of the disturbances in order to compute the control sequence that minimises a given cost function over the optimisation horizon. This cost function can combine comfort level and energy consumption. This paper presents the application of optimal control to auxiliary heating of a passive solar commercial building. Simulation-based and experimental results show that it can lead to significant energy savings while maintaining or improving the comfort level in this type of building.

1. INTRODUCTION

Modern office buildings are often characterised by a high level of internal gains due to intensive use of electrical appliances. In the case of passive solar buildings, but also for many recently designed buildings, important solar gains also contribute to lessen the heating load already reduced by a good thermal insulation. The share of heating cost in the total operation cost of this type of building is usually very low. However, energy savings can still be realised by a better control strategy. Furthermore, this high level of uncontrolled gains can lead to uncomfortable overheating periods, even during the heating season. A ‘‘smart’’ heating control strategy should take both concerns into account in order to minimise occupants discomfort while keeping the energy consumption as low as possible.

Optimal control of auxiliary heating plant in solar buildings was considered by different authors in the 1980s (Winn and Winn, 1985; Rosset and Benard, 1986). These papers present simulation-based results using simple models for the building and HVAC plant. They show that substantial energy savings and comfort improvement can be achieved. Later works of André and Nicolas (1992) and Fulcheri *et al*. (1994) show that these gains are significantly reduced when they are evaluated on more complex models and a fortiori on real buildings, if the internal model of the controller is too simple.

Interest for optimal control rose again in the 1990s, mainly for cooling applications. Braun (1990) considers an entire cooling plant and one building zone, to study the possible energy and cost savings of optimal control compared to conventional night set-up control. A parametric study covering a wide range of conditions is made with synthetic weather data and considering ‘‘steady periodic’’ solutions. Keeney and Braun (1996) show that a large fraction of these energy cost savings can be obtained with a simplified control strategy. The optimisation of two control variables (e.g. pre-cooling period and power), combined with a classical comfort-based controller with simple rules during building occupancy, can yield about 95% of possible cost savings using optimal control. This solution drastically reduces the computational load of the optimisation.

In cooling applications, achievable cost savings are rather impressive, taking advantage of the time-of-day electricity rate. The real energy con-

†Author to whom correspondence should be addressed. Tel.: +32-63-230-858; fax: +32-63-230-800; e-mail: andre@ful.ac.be

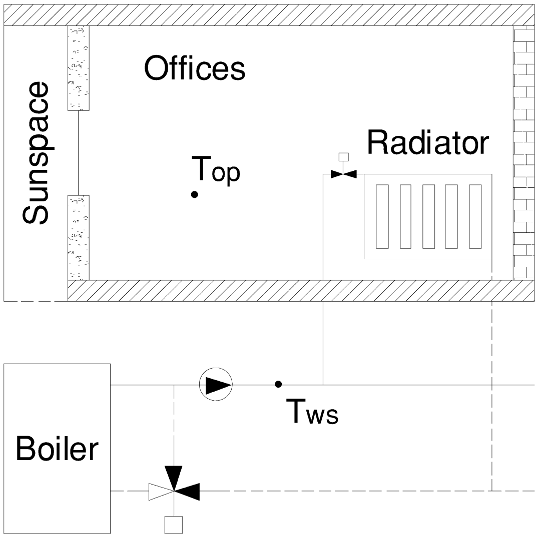

Fig. 1. Considered system..

sumption is only slightly reduced, or even increased. In the case of non-electrical heating, achievable cost savings are less impressive but they are always combined with real energy savings. This paper shows that thermal comfort can be improved while reducing the energy consumption in comparison with a classical controller, which makes optimal control doubly interesting.

2. CONSIDERED SYSTEM

The system, shown in Fig. 1, includes a part of the building and the heating installation. The considered building part consists of one thermal zone of a passive solar commercial building. This zone consists of two offices (30 m^2), which are adjacent to a south facing sunspace. The sunspace is 1 m deep and totally glazed. It is separated from the offices by a mass wall (heavy concrete, 25 cm) including 10 m^2 internal windows. External windows (2 m^2),which can be opened by occupants, are also present in offices. The hot water heating system includes a boiler, a three-way valve and a radiator. The control variable is the water supply temperature, T_{ws}. In the reference case, a thermostatic valve is present on the radiator. This valve is maintained fully opened in the case of optimal control. The controlled variable is the operative zone temperature in offices (T_{op}).

3. OPTIMAL CONTROL ALGORITHM

The principle of optimal control is to use a model of the system and a forecasting of future disturbances to compute the control sequence that minimises a given criterion, the cost function. This objective function is minimised over the optimisation horizon, which must be large enough to allow an efficient anticipation of disturbances.

Fig. 2 presents the scheme of the implemented optimal controller. Its principle is briefly described here under. Further details on different ‘‘blocks’’ are given in Sections 3.1–3.7.

1. At each time step (0.25 h) some variables are measured: zone operative temperature (T_{op}), radiator supply and return temperature (resp. T_{ws} and T_{wr}), ambient temperature (T_{amb}) and solar radiation on southern façade (G_S).
2. These variables are passed to three different subsystems:

   System identification routine. The parameters of the building and heating plant simplified model are corrected taking into account the latest measurements on the system.

   Kalman Filter. It estimates the state of the simplified model included in the optimal

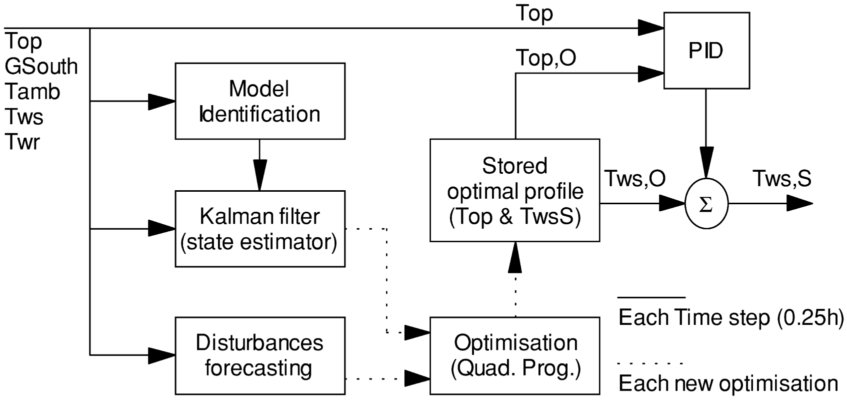

Fig. 2. Optimal controller block scheme.

controller. This allows the use of a good quality estimation of initial conditions for the optimisation.

Disturbances forecasting algorithm. It predicts the ambient temperature and solar radiation for the next optimisation period (e.g. 24 h).

3. At the beginning of each new optimisation period, the optimisation algorithm minimises the cost function on the given horizon (N_H), giving a 0.25 h-profile of T_{op} and T_{ws} (respectively $T_{op,O}$ and $T_{ws,O}$). It uses the estimated state of the system, the newly identified parameters and the disturbances forecasting.
4. A PID controller tracks the setpoint for T_{op} ($T_{op,O}$), correcting the optimal water supply temperature ($T_{ws,O}$). Its output is the setpoint for the water supply temperature ($T_{ws,S}$).

3.1. Simplified model

The linear state-space building model, based on a second-order wall representation, was developed for control purposes and is presented in an earlier paper (Kummert *et al.*, 1996). It has been optimised to realise a compromise between accuracy and complexity. The global building model includes 2 air nodes and 4 walls, which gives 10 state variables. It can be represented by a ‘‘star’’ network of thermal resistances and capacitance’s, where each wall makes one branch connecting the air node to other nodes (e.g. ambient temperature or adjacent zones). A simplified representation of the building simplified model is shown in Fig. 3.

The radiator is modelled as a single node and heat emission characteristics are linearised. The average temperature between radiator (T_R) and water supply (T_{ws}) is used to compute the power emission. Heat flux is directed to air and to wall surfaces according to a fixed ratio. The simplified model only takes into account the inertia and the maximal power of the boiler (a constant efficiency is assumed), and pipes are neglected.

3.2. System identification

The building and heating plant model contains 52 parameters, which are directly or indirectly related to physical properties. These parameters represent thermal conductance’s and capacitance’s, or solar radiation transmittance’s, etc. Due to the simplified nature of this model, some parameters have to be identified online in order to reproduce the behaviour of the real system. However, this number of parameters is rather high for a so-called ‘‘simplified’’ model and a ‘‘rough’’ simultaneous identification of all parameters is not likely to converge to a good solution.

The initial value of all parameters is determined by simplification of the physical laws governing heat transfer: conduction, convection, radiation. This allows obtaining reasonable values for these parameters, which give a good approximation of the real system. The parameter identification takes this fact into account by considering these values as ‘‘nominal’’ and attracting the identified parameters towards their nominal values. Furthermore, physical considerations are used to restrain the

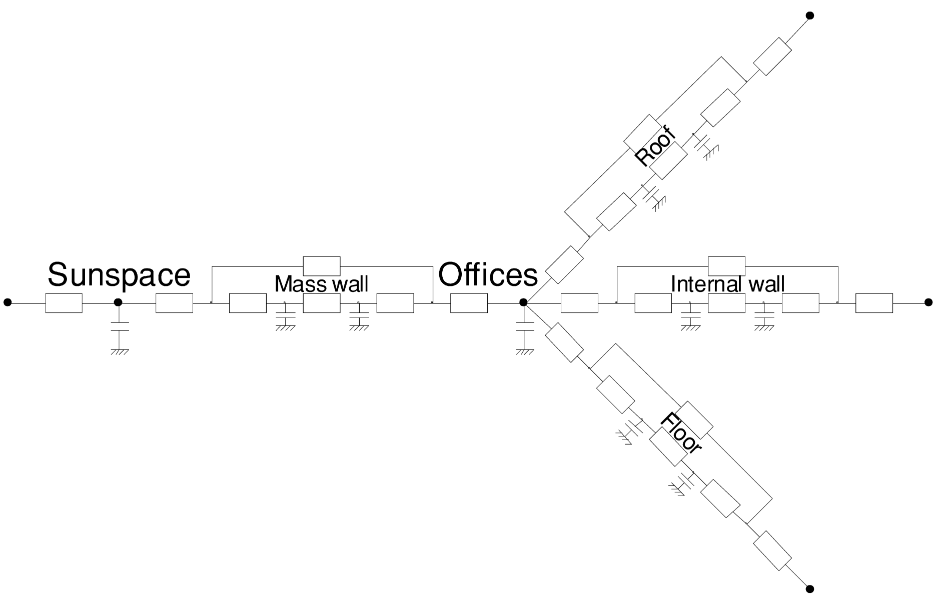

Fig. 3. *R–C* representation of thermal building model.

possible range of every parameter (e.g. a conductance must be positive).

The parametric identification uses a prediction error method. It is realised in two distinct steps:

First, the data measured over a long period (e.g. 1–3 weeks) is used to identify a constant value for each parameter, ‘‘attracting’’ the parameters towards their nominal value. The minimised criterion (Vl) is:

$$Vl = \sum_{i=1}^{N} e^2(t_i) + \sum_{j=1}^{Np} w_j (G_{R,j} - 1)^2 \quad (1)$$

with e model error on T_{op} (simulated – measured); w_j weight of parameter j in the criterion; $G_{R,j}$ normalised value of parameter j, defined by

$$G_{R,j} = G_j / G_{Nom,j} \quad (2)$$

where $G_{Nom,j}$ is the nominal value for parameter j.

Secondly, the four last time steps (1 h data) are used to identify some parameters that are likely to vary with a small time constant due to a variation in the real system (e.g. infiltration rate is dependent on windows opening) or due to simplification hypothesises (e.g. incorrect evaluation of glazing optical properties, linearisation of radiative heat fluxes).

In this case, only some parameters are identified, the other ones being ‘‘frozen’’ to the values obtained during the first identification process. The minimised criterion is simply the prediction error criterion (first term of Eq. (1)).

3.3. State estimator

The model initial state must be estimated at the beginning of each optimisation period. The initial values of all state variables in the simplified model must be known. These variables cannot be measured on a real system and the Kalman filter is a simple and effective way to estimate them from the measured outputs.

The state estimator uses the measured zone temperature (T_{op}) and measured inputs and disturbances: radiator supply and return water temperature (resp. T_{ws} and T_{wr}), ambient conditions (G_S and T_{amb}). The internal model of the Kalman filter uses the latest parameters values obtained by the system identification phase.

3.4. Cost function

The cost function must be an expression of the trade-off between comfort and energy consumption. The chosen indicator of thermal comfort is Fanger’s *PPD* (Fanger, 1972), while energy cost is considered to be proportional to the boiler energy consumption (Q_b). In the discomfort cost, *PPD* is computed with default parameters for non-measured aspects (air velocity, humidity and metabolic activity). Furthermore, it is assumed that occupants can adapt their clothing to the zone temperature. This method allows modelling a comfort range in which occupants are satisfied. With the chosen value for parameters, the comfort zone covers operative temperatures from 21°C to 24°C. *PPD* is also shifted down by 5%, to give a minimum value of 0. This modified *PPD* index will be referred to as *PPD′*. Discomfort cost function is represented Fig. 4.

This gives, respectively for discomfort cost and energy cost (J_d and J_e):

$$J_d = \int (PPD[\%] - 5) \quad (3)$$

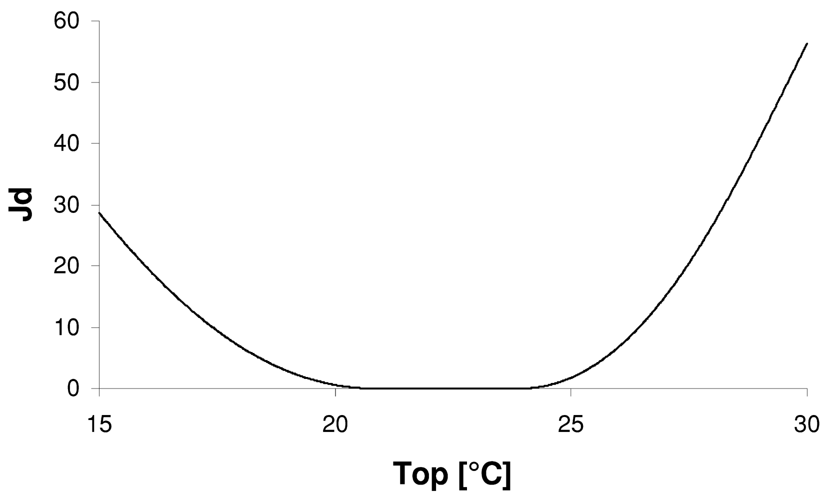

Fig. 4. Discomfort cost function.

$$J_e = \int \dot{Q}_b \quad (4)$$

The global cost (J) is a weighted sum of both:

$$J = \alpha J_d + J_e \quad (5)$$

The global cost function implemented in the controller is a quadratic-linear function, where the quadratic term is an approximation of PPD' and the linear term is exactly J_e. It is detailed in an earlier paper (Kummert *et al*., 1997). The cost function used to assess the controller performance and to compare it with conventional solutions includes the exact value of PPD'.

3.5. Disturbances forecasting

Internal gains are related to occupancy schedules, which are well known in office buildings. For meteorological disturbances, different solutions were alternatively implemented.

The simplest prediction method for solar radiation and temperature with a short-term horizon (24 h) is to use the values of the previous day. The obtained forecasting quality is of course not very good.

An attempt was made to use local measurements of solar radiation, temperature, humidity and other meteorological variables. The local-based forecasting was realised using Artificial Neural Networks combined with classical time series analysis methods. This study showed that an improvement of the forecasting quality can be achieved compared to the ‘‘previous day’’ approach (Kummert *et al*., 1998). However, the involved computational power is important with respect to the quality improvement and this solution was not retained for the real implementation.

The second retained option is to use weather data delivered by a meteorological server. These forecasts are computed by powerful computers using global weather information and can be of very good quality. We used the information delivered to the agricultural sector by the Belgian Royal Meteorological Institute (IRM-KMI). Forecasts for 10 meteorological parameters (including temperature, humidity and solar radiation) are sent by email twice a day, with a forecasting horizon of 36 h. Data is available for 21 different regions in Belgium.

Finally, in simulation, perfect forecasting were used as well to assess the influence of forecasting quality on the controller performance.

3.6. Optimisation algorithm

The problem of finding the control sequence minimising a linear-quadratic cost function for the given linear system can be rewritten as a quadratic-programming problem (Kummert *et al*., 1997). This guarantees the existence of a solution and allows the use of efficient projected gradient algorithm. This algorithm was implemented in Matlab Optimisation Toolbox, which was used for the optimal control computation (Grace, 1996).

The system includes 11 state variables, which correspond to the nodes of the simplified model (2 air temperatures, 8 wall temperatures and the radiator temperatures). For a 24 steps-ahead optimisation, the total number of variables in the QP-problem is 325, and 397 linear constraints are necessary. Typical computational time is about 40 s on a Pentium II-350 PC, using Matlab (a C++ equivalent code should run much faster). Memory requirements are not too high since most matrices are sparse.

In the case of perfect modelling and perfect disturbances forecasting, the optimisation should be repeated only at the end of the period on which the cost function was minimised. However, to reduce the influence of modelling and forecasting errors, a ‘‘receding horizon’’ is used, i.e. the optimisation is repeated with a period shorter than the prediction horizon. In this study, optimisation horizons ranging from 16 to 24 h were considered and the optimisation was repeated up to every hour (range: 1–6 h).

3.7. PID controller

When a new optimisation is computed, a feedback from the real system is present, since the estimated state of the system based on measured outputs is used. During the period between two optimisations, the computed optimal control profile is applied without any feedback from the real system. In the case of large forecasting errors, this can lead to a system evolution being far from the predicted one and hence far from ‘‘the optimum’’. To compensate for these errors, a feedback controller is cascaded with the optimisation. This controller is a conventional PID with anti-windup and uses the base time step (0.25 h).

4. SIMULATION RESULTS

The controller was implemented in a simulation environment including reference models for the building and the heating plant. This environment combines TRNSYS and Matlab software’s. The role of the real system is played by different models implemented in TRNSYS. The optimal controller is implemented in Matlab. The communication between TRNSYS and Matlab is realised by a special TRNSYS TYPE calling the Matlab Engine Library. This simulation environment is described in an earlier paper (Kummert and André, 1999). These simulations tests allowed to tune some parameters of the controller and to assess its performance in comparison with a conventional control strategy. All simulations concerned a passive solar building characterised by an important south-facing glazed area and by a high thermal inertia. Some significant results are presented here under.

4.1. Comfort/Energy trade-off

The cost function implemented in the optimal controller is presented in Section 3.4. α (see Eq. (5)) is a parameter that allows to give more or less importance to comfort versus energy consumption. As above-mentioned, the discomfort cost (J_d) implemented in the controller is an approximation of PPD'. This value is integrated and can be expressed in [%h]. If we express the energy cost (J_e) in kWh, α units are [kWh/%h]. α can thus be interpreted as ''the energy quantity (expressed in kWh) that we accept to consume to reduce the percentage of dissatisfied people in the building by 1% during 1 h''.

Fig. 5 compares the total energy consumption and integrated PPD' for different α values in the range [1;10]. It can be seen that the ratio between total energy consumption and integrated value of PPD' on a long period is not equal to α. However, this parameter represents a simple way to obtain different comfort/energy trade-offs

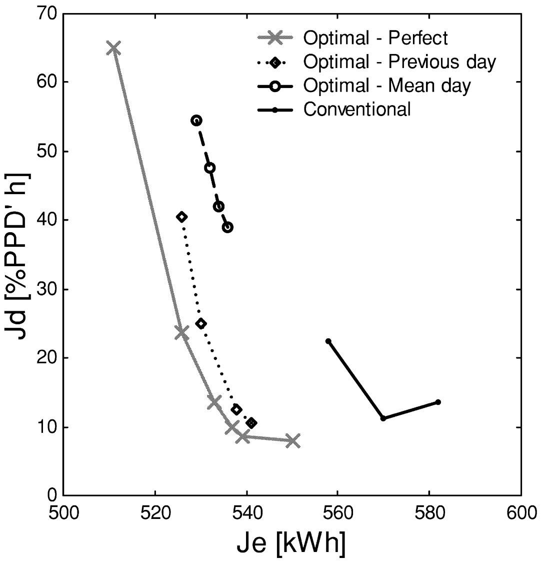

Fig. 6. Influence of the forecasting quality.

4.2. Forecasting quality

Fig. 6 represents the global performance of the optimal controller with different forecasting types: perfect forecasting, use of the previous day and use of a mean day (poor quality forecasting). This plot represents J_d versus J_e. The closer a controller is to the lower left corner, the better its performance is. The performance of a conventional controller is also presented. This controller is

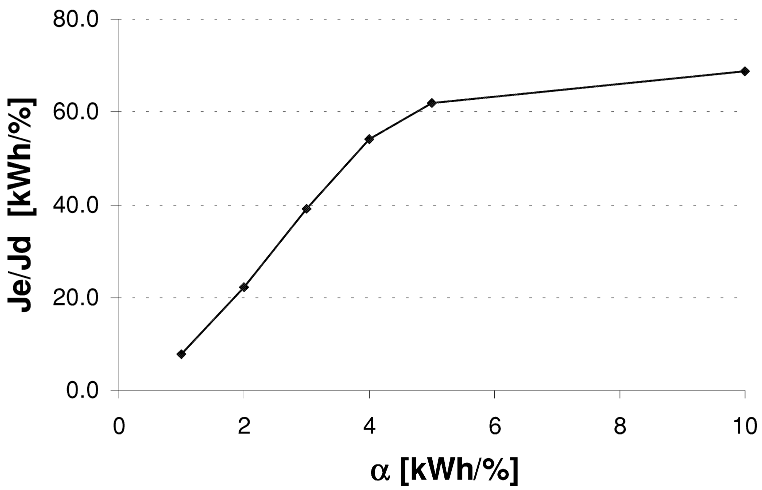

Fig. 5. Comfort/Energy trade-off.

based on a combination of a heating curve with thermostatic valves and makes use of a simple optimal start algorithm (Seem *et al*., 1989).

Different values of α are used (1 to 5) for each forecasting case. The performance decrease resulting from the use of ''previous day'' forecasting is not too important: for a discomfort about 12, the energy consumption rises from 533 to 538, which represents a 1% increase. The difference increases for lower α values (higher part of the plot). This can be explained by the greater freedom left to the controller for small α values: achievable gains are more important in this case, but the optimal zone temperature profile is very dependent on meteo conditions. In this case, a forecasting error has a larger influence. The comparison with the conventional controller shows that the optimal controller still gives a better performance despite imperfect forecasting. In the case of ''mean day'' forecasting, the controller performance is quite poor, and low discomfort cost values cannot be attained.

This comparison shows that the quality of meteorological forecasting is an important factor for the controller but it also shows that the use of the previous day seems to be a satisfying solution.

5. EXPERIMENTAL RESULTS

The optimal controller was implemented in a real building on the university campus. Two offices were selected to play the role of the reference zone. All system's variable (internal, external and water temperatures, flow-rates, solar radiation) were recorded during two heating seasons. The operative temperature of each room was measured by a special sensor presenting a relative sensitivity to radiation and convection close to the one of a human body.

5.1. Compared controllers

5.1.1. Conventional controller. The implemented algorithm mimics the existing heating control scheme in the building. The water supply temperature is controlled by a heating curve varying according to a fixed schedule. The heating curve is designed to maintain 21°C during day and 15°C during night (or week-ends). Thermostatic valves are placed on each radiator and set by building occupants according to their preferences.

The good practice when choosing the heating curve in such installations is to overestimate the ''day'' curve in order to allow a quicker warm-up of the building, leaving to the thermostatic valves the role to maintain indoor temperature below their setpoint. The night heating curve can be slightly underestimated since the building will almost never meet steady-state ''night'' conditions, but this is not often done.

5.1.2. Reference controller. This controller realises a purely thermostatic control acting on the water supply temperature to maintain the desired temperature in the reference room. The thermostatic valves are removed in this room. A fixed schedule is used to allow a pre-heating time before occupancy.

The main advantage of this controller, compared to the conventional one, is that it does not assume a steady-state of the building. This will result in the maximum usage of boiler power for pre-heating, which allows for a less conservative fixed schedule, and this will effectively switch the heating off during night, as long as the night setpoint is exceeded. Combining a more efficient night setback and a later start of the heating, this controller can lead to significant energy savings compared to the conventional one, without requiring much intelligence in the algorithm. In practice, the thermostatic control is realised by a PID algorithm acting on Tws.

5.1.3. Optimal controller. This controller has been described in details in previous sections. A mid-range comfort level ($\alpha = 6$–7 in Eq. (5)) was applied most of the time. Some tests were made with higher values, but no significant difference was noted. Lower comfort settings values were not implemented to maintain the temperature in an acceptable range for building occupants, who considered the retained ''comfort temperature'' (21°C) as ''rather cold''.

Meteorological forecasts provided by IRM (Royal Meteorological Institute of Belgium) were used during half of the optimal controller testing period instead of local-based forecasting. The latter was actually reduced to the use of previous day data as forecasts, as the neural network approach did not give satisfying results.

5.2. Typical daily profiles

The next figures (Figs. 7–11) represent typical profiles of the following variables: T_{op}: operative temperature in reference offices; T_{ws}: Water supply temperature; T_{wr}: Water return temperature; Q_r: Radiator emission power; T_{amb}: Ambient

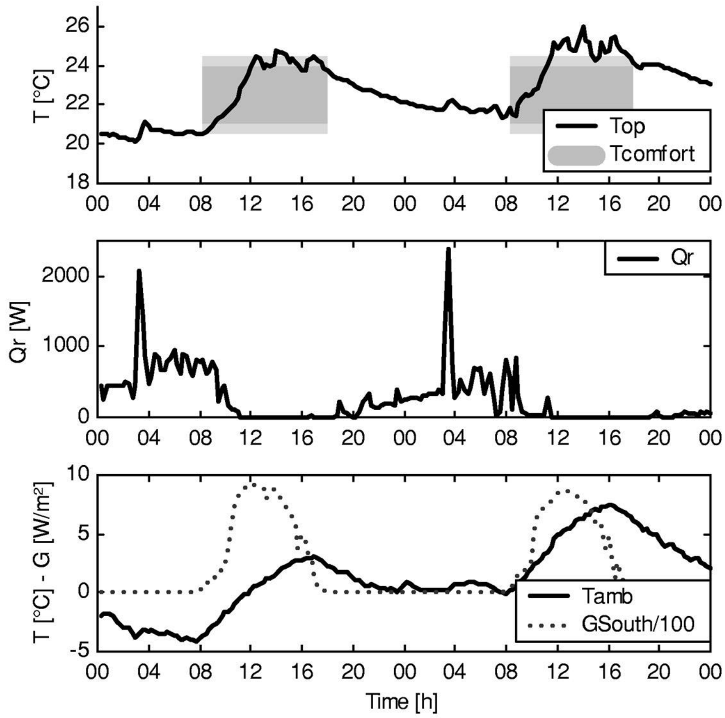

Fig. 7. Sunny days, conventional controller.

temperature; G_{south}: Solar radiation on southern façade

Grey rectangles represent the comfort temperature range (21–24°C) when building is occupied (from 8 AM to 6 PM). The discomfort cost is zero in this temperature range. Light grey rectan-

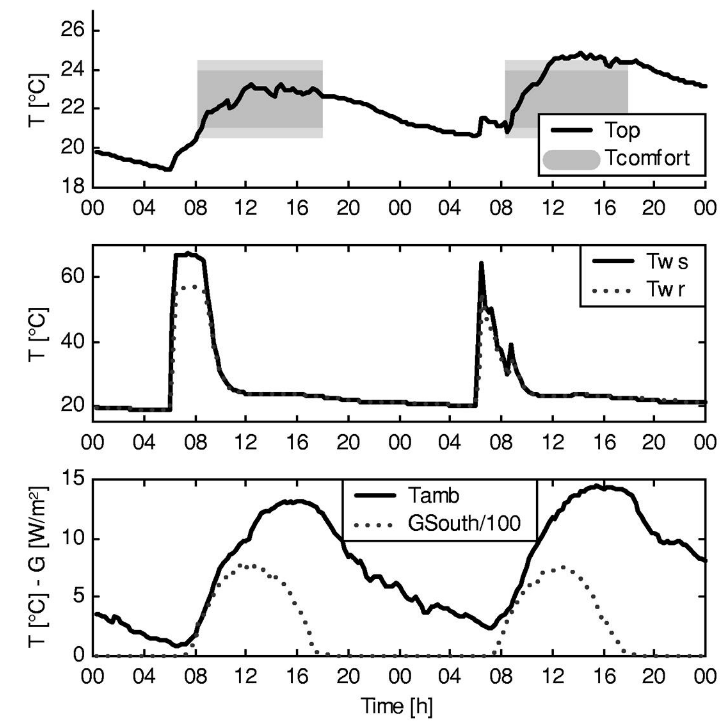

Fig. 8. Sunny days, reference controller.

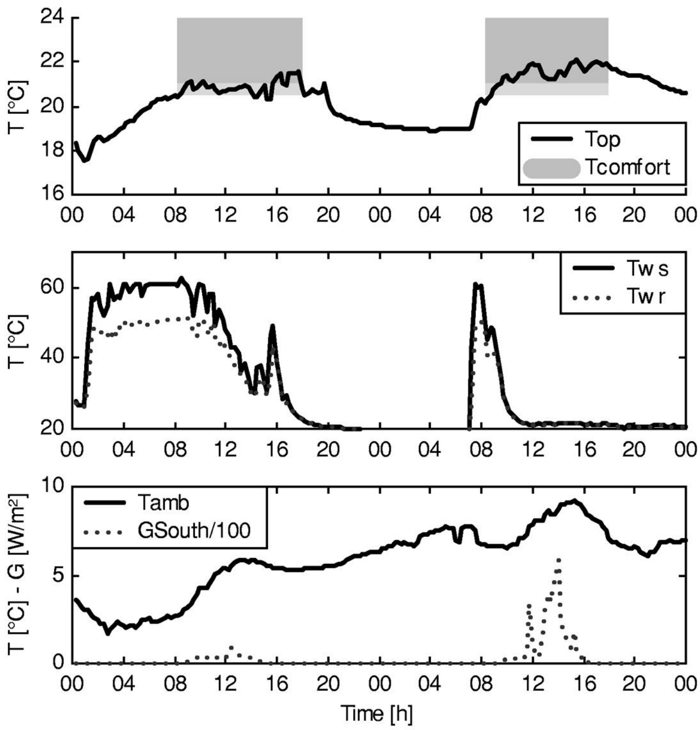

Fig. 9. Typical Monday and Tuesday, optimal controller.

gles next to them indicate the zone where comfort is still very low (i.e. 0.5°C below the lower limit and 0.5°C above the upper limit).

T_{ws} and T_{wr} are represented for the reference and optimal controller because they show the controlled variable (T_{ws}), while Q_r is used for the

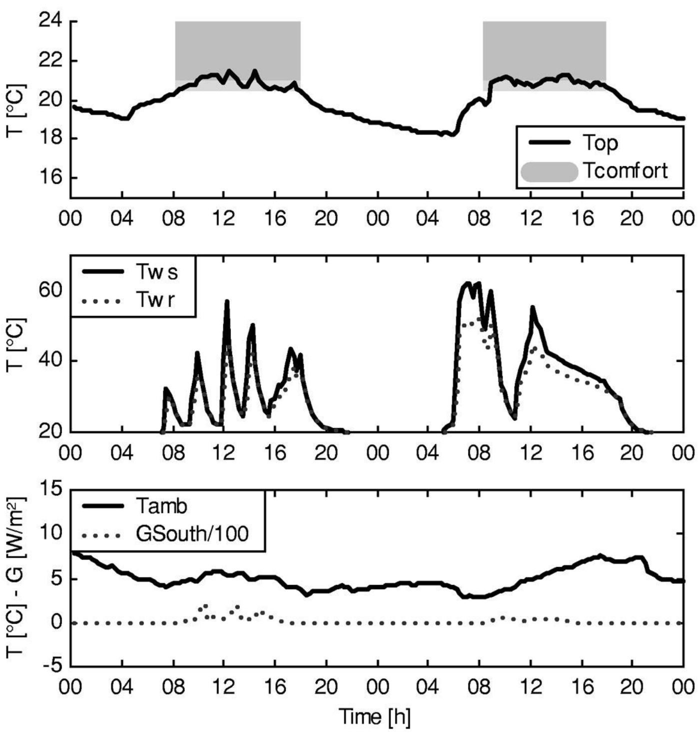

Fig. 10. Cold and cloudy days, optimal controller.

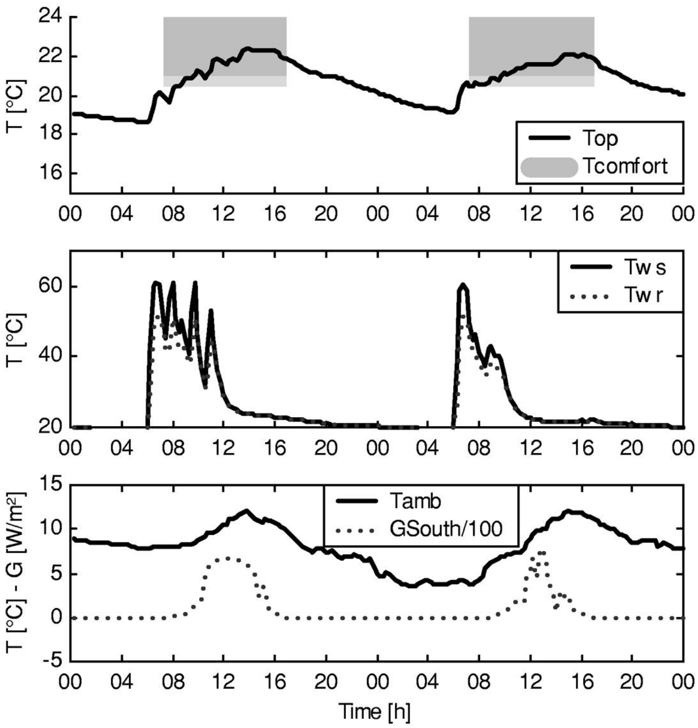

Fig. 11. Sunny mid-season days, optimal controller.

conventional controller. Thermostatic valves control the flowrate in radiators, so this power would not be accurately represented by the temperature profile alone.

5.2.1. Conventional controller. Fig. 7 shows that important overheating can occur in the building when the conventional controller is implemented.

The fixed heating schedule cannot be adapted to all conditions and is too conservative if the building has been submitted to high solar radiation during some successive days. It is the case for this period: heating is started at 3AM, which is a good compromise for this time of the year (February). However, the building is very warm already. The thermostatic valves close quite quickly (reacting not only to the zone temperature but also to the radiator temperature itself), but the zone is nevertheless heated to about 21°C before occupants arrive.

During the day, internal and solar gains lead to overheating and to discomfort. Note that overheating occurs even if the windows are open. It can be seen on the graph that the increase of temperature is suddenly slowed down around 13:00 or 14:00, due to windows opening. It is also very interesting to note that users open the windows when the temperature is already outside the comfort range, in other words when it is too late.

5.2.2. Reference controller. Fig. 8 presents two sunny mid-season days, when the reference controller was implemented.

The applied heating schedule is not too conservative for the concerned period, which can be seen the first day: the desired temperature is reached just after the theoretical occupation start.

However, after this sunny day, the building structure is significantly warmer and the required pre-heating time is far less important during the second day. The temperature is at the desired level at occupancy start, but increases immediately after and overheating occurs in the afternoon.

This phenomenon is less important than for the conventional controller (for which the thermostatic valve proportional band causes the heating to stop later), but it is still present.

It can be seen again that the occupants open the windows when the temperature reaches the upper comfort limit, interrupting the temperature raise, but too late.

5.2.3. Optimal controller. Fig. 9 shows temperature profiles for two typical winter days (Monday and Tuesday). It can be seen that the optimal controller starts heating at the latest moment to reach an acceptable temperature when occupants are supposed to enter the building. During occupation, the heating is reduced earlier than in the case of conventional heating (thermostatic valves or PID) because internal and solar gains are anticipated.

Fig. 8 shows Temperature profiles for two cold and cloudy days. The first day shows an influence of the PID correction. If the forecasted zone temperature is not maintained with the foreseen water supply temperature, a correction is applied to maintain the desired zone temperature. To prevent unnecessary overheating, this correction is not applied if the temperature lies between comfort bounds. During this day, the foreseen temperature was higher than the real one, because of overestimated solar radiation forecasts. The PID does not track this temperature if the real temperature lies within the comfort range, but well if it lies outside. This can lead to oscillations in the water supply temperature if the zone temperature is close to the lower comfort bound.

The second day of Fig. 10 shows a typical ‘‘end of day’’ profile: the radiator temperature drops since 12 PM and the zone temperature falls just below the comfort level at the end of the occupation period. This allows to save heating energy, but it is sometimes not appreciated by buildings occupants (see the ‘‘users point of view’’ section).

Finally, the building behaviour during relatively warm and sunny days is presented Fig. 11. This figure can be compared to Figs. 7 and 8. The optimal controller allows to save both energy and discomfort in the case of high solar gains leading to overheating. The two means that can be used to obtain this result are:

Delay the heating start to reach the comfort temperature at the latest moment or even just after due time, to maintain a colder building structure.

Maintain the temperature slightly below the comfort range during the early morning in order to decrease the maximum temperature reached in the afternoon.

6. PERFORMANCE COMPARISON

The available experimental facility did not allow the simultaneous implementation of different controllers. Furthermore, it would have been almost impossible to obtain a similar user behaviour in two different reference rooms, and users have a strong influence on the thermal behaviour of the building by opening or closing the windows.

Different controllers were alternatively implemented in the same building, during two heating seasons (1998–2000). The global performance of different controllers cannot be compared directly, as meteorological and user behaviour characteristics were different for each of them. The performance comparison will be based on two different techniques:

- consideration of ‘‘short’’ periods (2–4 weeks) presenting similar weather and occupancy conditions
- use of simulation to compute the performance of controllers that were not implemented

6.1. Comparison on short periods

The first comparison concerns the conventional and optimal controllers, for which two similar 2-weeks periods are considered.

Table 1 shows the summary of relevant meteorological parameters and of both controllers performance during the retained period. The weather conditions are representative of rather warm and sunny mid season periods. These results are obtained on relatively short periods, but can still give a good idea of the relative performance of both controllers.

The conventional controller uses a fixed schedule. During relatively warm periods, this schedule is too conservative, which leads to waste energy to pre-heat the building too long in advance. Furthermore, this warm building is more subject to overheating. This last point is still reinforced by the proportional band of the thermostatic valves, which reduce the power when the temperature reaches the setpoint but do not really stop the heating until the temperature is about 0.5°C above this setpoint.

In this kind of situation, the optimal controller is able to reduce the energy consumption while reducing the discomfort. Energy savings on the considered period reach 13%, for a significantly

Table 1. Weather, comfort and energy parameters, optimal and conventional controllers, sunny mid season period

		Conventional	Optimal
T_{amb} [°C]	Min	2.0	3.5
	Max	18.7	17.2
	Avg	10.0	9.3
G_S [W/m^2]	Avg	67	62
J_d [%PPD']	Max	3.8	2.4
	Avg	0.25	0.07
PMV' [–]	Min	−0.13	−0.34
	Max	0.43	0
	Avg	0.04	−0.02
P_{heat} [kW]	Avg	0.175	0.152

reduced discomfort (‘‘optimal’’ discomfort cost is 28% from ‘‘conventional’’ cost).

The second comparison concerns the optimal and the reference controller. Table 2 again shows the summary of relevant meteorological parameters and of both controllers performance during the retained period. The weather conditions are representative of cold winter periods.

During this cold period, the fixed schedule leads to energy waste on some days because the pre-heating time is too long, but to high discomfort on other days because the pre-heating time is too short. The optimal controller sometimes underestimates the pre-heating time as well, leading to relatively high discomfort, but it adapts this pre-heating time to the building state. On the whole period, this allows here again to reduce the discomfort while saving energy (about 12% energy savings with 44% discomfort cost reduction).

6.2. Comparison using simulation

The performance of two controllers on the same building can be compared using mixed experimental and simulation results. The principle is as follows:

- During a first period, the controller one is tested on the building.
- During a second period, the controller two is tested on the building.
- The simulated performance of controller one on the first period and the simulation of controller two during the second period are used to validate a building model for the considered meteorological data set.
- In a second step, the performance of controller one during the second period and the performance of controller two during the first period are simulated and serve to establish a virtual comparison on the same periods.

This method can be used to refine the comparison between different controllers implemented on one single building.

However, the simulation of really implemented controllers does not reproduce accurately enough their performance with the simulaton environment described here above, due to building modelling errors in the reference model (TRNSYS TYPE 56). Different reasons can explain this:

- The desired accuracy is quite high, since the objective is to quantify performance differences (energy consumption and comfort index). Errors of 5–10% are often considered as a good model accuracy in common practice, but they do not allow to quantify performance differences of the same order of magnitude.
- Some complex interactions with other zones of the building, including air movements, are not correctly modelled
- Very important heat losses from the boiler room and from pipes cause high unmeasured heat gains to the reference zone. This has been clearly pointed out by the difference between summer and winter performance and by two boiler failures. Indeed, the building response is far more accurately simulated when the boiler is not in operation. These losses are dependent from a second heating circuit which is not modelled.

Note that this accuracy problem does not imply that the simulation results presented in Section 5 are not interesting. Indeed, previous work such as IEA Annex 21/Task 12 (Lomas, 1994) showed that most building simulation programs often better reproduce the influence of design changes on energy and comfort performance than the absolute performance. This ability to reproduce the relative performance more accurately than the absolute results can be extrapolated to our application (controller change and not design change). The results obtained in the ‘‘pure’’ simulation phase can then be considered as giving a realistic idea of controllers performance when compared to each other.

For the simulation-based/experimental comparison, a simplified model similar to the internal model of the controller was used. It allows to identify more easily some varying parameters (e.g. infiltration rate) and other poorly known influences (e.g. unmeasured heat gains).

Tables 3 and 4 illustrate obtained results when comparing the conventional controller and the optimal controller on two 1-month periods presenting different meteorological characteristics and using the identified model to extrapolate the performance comparison.

Table 2. Weather, comfort and energy parameters. Optimal and reference controllers, cold winter period

		Reference	Optimal
T_{amb} [°*C*]	Min	−4.1	−8.3
	Max	9.1	8.2
	Avg	1.1	1.3
G_S [W/m^2]	Avg	27	26
J_d [%*PPD*′]	Max	6.1	3.1
	Avg	0.25	0.14
PMV′ [−]	Min	−0.55	−0.39
	Max	0	0
	Avg	−0.04	−0.03
P_{heat} [kW]	Avg	0.403	0.356

Table 3. Weather, comfort and energy parameters. Period 1

	Conventional measured	Conventional simulated	Optimal simulated
$T_{amb\ min}$ [°C]	−1.4	−1.4	−1.4
$T_{amb\ max}$ [°C]	18.7	18.7	18.7
$T_{amb\ avg}$ [°C]	7.0	7.0	7.0
$G_{south\ avg}$ [W/m^2]	111	111	111
$J_{d\ max}$ [%PPD']	13.0	10.2	5.4
$J_{d\ tot}$ [%PPD' h]	280.5	262.6	215.0
$J_{e\ tot}$ [kWh]	130.5	135.0	111.6

The first part of each table sums up the meteorological parameters of the considered period. Comfort and energy parameters are given:

1° as measured on the real building (with conventional controller for period 1, with optimal controller for period 2)

2° as simulated for the controller that was really applied (model validation)

3° as simulated for the other controller

The results show a very good agreement between simulation and experiments: the energy performance is reproduced within 3.5%. The larger error on the discomfort cost (6% on total, 27% on maximum value for 0.25 h) is due to the non-linear shape of the cost function, which amplifies the error on operative temperature (see Fig. 2).

The comparison shows that energy savings of 20% can be achieved during the first period (sunny mid season) while improving the thermal comfort by 18%. During the cold period 2, energy savings of 7% can be achieved with a maintained thermal comfort (small increase of discomfort: 2%).

Simulations on the entire heating season show important energy savings (15–20%) for an improved thermal comfort. Furthermore, energy savings in the range of 10% can be achieved as well compared to the ‘‘reference controller’’, with a similar thermal comfort.

6.3. User's point of view

A real user survey about the comfort in the test building was out of the scope of this work. However, the two regular occupants of reference offices were given survey forms where they could write their complaints when they felt uncomfortable. They were also surveyed on a regular basis to give their opinion on the thermal and general comfort in the building. Some information can be gained from these surveys and from the few complaints that occurred. Note that these occupants were not at all involved in the project nor working in the field of building energy management.

The first conclusion of this small survey is that the comfort feeling is not always directly related to the temperature that is measured by the controller. Many objective and subjective factors can have an influence: humidity, draughts, occupants mental/physical state, . . .

In this respect, a controller achieving perfect thermal comfort for all occupants is not realistic.

However, some typical user behaviours could be considered in the development of a commercial controller:

- If building occupants feel uncomfortable, their first reaction is to verify that the radiators are cold/warm according to what they desire. It is also very often the case that they verify if the radiators are warm when they arrive in the building on a cold winter morning. In this respect, the optimal controller was appreciated because the heating is started as late as possible and the water temperature is very often high when the occupants arrive.
- On the other hand, it happened quite often that

Table 4. Weather, comfort and energy parameters. Period 2

	Optimal measured	Optimal simulated	Conventional simulated
$T_{amb\ min}$ [°C]	−7.3	−7.3	−7.3
$T_{amb\ max}$ [°C]	17.2	17.2	17.2
$T_{amb\ avg}$ [°C]	4.6	4.6	4.6
$G_{south\ avg}$ [W/m^2]	51	51	51
$J_{d\ max}$ [%PPD']	6.7	4.9	3.02
$J_{d\ tot}$ [%PPD' h]	199.5	194.2	190.1
$J_{e\ tot}$ [kWh]	190.5	196.6	211.2

the occupants were feeling cold on a cloudy afternoon and did not appreciate the fact that radiators were cool. With a conventional heating curve control associated with thermostatic valves, they always have the possibility to increase the radiator temperature and the lack of such a possibility was probably the major disadvantage of the optimal controller. The comfort temperature setting does not play exactly the same role, as the real desire of the occupants often is to feel the warmth from the radiator rather than to have a warmer office.

Concerning the overheating problem, the optimal controller showed a very good behaviour. Moreover, simulation results confirm that this controller could be suitable even during very warm mid-season periods (when no heating is really needed), while the conventional controller would probably always heat the building in the morning. The need for user adjustment of the heating curve is completely suppressed.

7. CONCLUSIONS

Experiments on a passive solar commercial building have confirmed the simulation-based study and show that the optimal controller can achieve significant energy savings compared to conventional controller with thermostatic valves and also compared to a perfect thermostatic control, while maintaining or improving the thermal comfort. Furthermore, choice is given to building users to privilege either the comfort or energy savings thanks to a simple parameter. Obtained energy savings for a maintained or improved thermal comfort are about 9%, which fulfills the objective mentioned in the ‘‘Energy, Environment and sustainable development’’ work programme of the EC Fifth Framework Programme (European Commission, 1999).

Practical limitations have also been enlighted, mainly concerning the required computational power and the a priori knowledge which is necessary to give suitable initial values for the parameters of the internal building model. These aspects have to be considered carefully in order to make this algorithm suitable for commercial applications.

Acknowledgements—This research work was partly funded by the European Commission, in the framework of the non-nuclear energy programme JOULE III (Contract JOE3-CT97-0076).

The authors also wish to thank the Belgian Royal Meteorological Institute (IRM-KMI) for providing weather forecasting data.

REFERENCES

André Ph. and Nicolas J. (1992) Application de la théorie des systèmes à la thermique du bâtiment. Problèmes de modélisation, d’identification, de contrôle. *Revue Générale de Thermique* **371**, 600–615.

Braun J. E. (1990) Reducing energy cost and peak electrical demand through optimal control of building thermal storage. *ASHRAE Trans*. **96**(2), 876–888.

European Commission (1999). Energy, environment and sustainable development. Programme for Research, Technology Development and Demonstration under the Fifth Framework Programme. Available on http://www.cordis.lu/fp5/src/t-4.htm.

Fanger P. O. (1972). *Thermal comfort analysis and application in environmental design*, McGraw Hill.

Fulcheri L., Neirac F. P., Le Mouel A. and Fabron C. (1994) Chauffage des bâtiments. Intermittence et lois de régulation en boucle ouverte. *Revue Générale de Thermique* **387**, 181–189.

Grace A. (1996). *Optimisation toolbox for use with Matlab 5.* The MathWorks Inc, Natick MA.

Keeney K. and Braun J.E. (1996). A simplified method for determining optimal cooling control strategies for thermal storage in building mass. *HVAC&R Research, 2*(1).

Kummert M., André Ph. and Nicolas J. (1996) Development of simplified models for solar buildings optimal control. In *Proceedings of ISES Eurosun 96 Congress, Freiburg, Germany*.

Kummert M., André Ph. and Nicolas J. (1997) Optimised thermal zone controller for integration within a Building Energy Management System. In *Proceedings of CLIMA 2000 conference*. *(CD-ROM), Brussels*.

Kummert M., André Ph., Guiot J. and Nicolas J. (1998) Short-term weather forecasting for solar buildings optimal control: an application of neural networks. In *Proceedings of EUFIT 98 congress, 7–10 Sept., Aachen, Germany, Vol 2*, Zimmermann H. J. (Ed.), pp. 868–872, Verlag, Mainz, Aachen.

Kummert M. and André Ph. (1999) Building and HVAC optimal control simulation. Application to an office building. In *Proceedings of the 3rd Symposium on Heating, Ventilation and Air Conditioning (ISHVAC 99) conference, 17–20 Nov., Shenzen, China,II*, pp. 857–868, Tsinghua University & Hong Kong Polytechnical University.

Lomas, K. J (Ed.). (1994). *Empirical validation of thermal building simulation programs using test room data*. IEA Task 12 & Annex 21 Final report, International Energy Agency.

Rosset M. M. and Benard C. (1986) Optimisation de la conduite du chauffage d’appoint d’un habitat solaire à gain direct. *Revue Générale de Thermique* **291**, 145–159.

Seem J. E., Armstrong P. R. and Hancock C. E. (1989) Algorithms for predicting recovery time from night setback. *ASHRAE Trans*. **95**(2), 439–446.

Winn R. C. and Winn C. B. (1985) Optimal control for auxiliary heating of passive-solar-heated buildings. *Solar Energy* **35**(5), 419–442.